Extended Abstracts of the 2003 International Conference on Solid State Devices and Materials, Tokyo, 2003, pp. 438-439

P2-14

A Simple Wide-Band MIM Capacitor Model for RF Applications and the Effect of Substrate Grounded Shields

Seong-Sik Song, Seung-Wook Lee, Joonho Gil, and Hyungcheol Shin[1]

Dept. of EECS, KAIST, 373-1, Guseong-dong, Yuseong-gu, Daejeon 305-701, Republic of Korea
Phone: +82-42-869-3459 Fax: +82-42-869-8590 E-mail: hcshin@ee.kaist.ac.kr
[1]School of EE, Seoul National University, San 56-1, Shilim-dong, Gwanak-gu, Seoul 151-742, Republic of Korea

1. Introduction

On-chip Metal-Insulator-Metal (MIM) capacitors are used as one of the most important passive components in many radio-frequency integrated circuits (RF IC's). The conventional model of the MIM capacitor shown in [1] describes the frequency-dependent series resistance as a constant value for all frequency range and hence has the strong deviation in the *Q*-factor in multi-GHz region. In this paper, we have proposed a simple model that can accurately describe the frequency-dependency of the series resistance for the MIM capacitor. In addition, we present the results for MIM capacitors with various substrate conditions including different shield materials.

2. Equivalent Circuit Model

Fig. 1 illustrates the top and cross sectional views of an MIM capacitor. The unshielded MIM capacitor has the P-substrate contacts placed with the distance d_p from the edge of MIM layer as shown in Fig. 1. The proposed equivalent circuit model of an MIM capacitor is shown in Fig. 2. Compared with the conventional model shown in [1], the frequency-independent element R_p is additionally used along with L_s to model simply the frequency-dependent series resistance, Re(Z_{series}), due to the skin effect of the conductor [2], [3]. Using the frequency-dependent element as reported in [4] complicates integration of the model in SPICE-compatible simulators [3]. In Fig. 2, C_s represents the main capacitance between MIM layer and metal-4. R_s and L_s are the parasitic series resistance and inductance, respectively. C_{ox} represents the parasitic oxide capacitance between the bottom plate and the substrate (or the shielding plate). R_{sub} is the parameter to model the resistance due to the lossy silicon substrate (or the shielding plate).

To verify the proposed model, we have carried out the direct parameter extraction with *Y*-parameters of MIM capacitors fabricated on a 10 Ωcm p-substrate in a 0.18-μm RF CMOS process. Here we used seven test structures (DUT-1 ~ DUT-7) with an identical capacitor size (20 × 20 μm^2) except for various substrate conditions to investigate the effect of the grounded shield (as shown in Table I). Two-port S-parameter measurements were performed in the frequency up to 20 GHz using an HP8510C vector network analyzer and on-wafer RF probes. Pad parasitics were eliminated with the de-embedding structure.

Assuming $\omega L_s << R_p$, Z_{series} in Fig. 2 can be written as

$$Z_{series} \approx R_s + \omega^2 L_s^2 / R_p + j(\omega L_s - 1/\omega C_s). \quad (1)$$

From the imaginary part of eq. (1), L_s and C_s can be directly extracted as shown in Fig. 3(a). R_p and R_s was also determined from the real part of eq. (1) as shown in Fig. 3(b).

With the assumption of $1 << \omega^2 R_{sub}^2 C_{ox}^2$, Y_{sub} in Fig. 2 was approximated as follows:

$$Y_{sub} \approx \omega^2 R_{sub} C_{ox}^2 + j\omega C_{ox}. \quad (2)$$

From eq. (2), the parasitic parameters C_{ox} and R_{sub} were simply extracted at low frequency using a linear regression.

Based on the direct extraction procedure, seven test structures were characterized and the values of six parameters shown in Fig. 2 were obtained. The extracted parameter values are summarized in Table I. Since ωL_s=10.56 Ω at 20 GHz and R_p=155 Ω in the worst-case, the assumption leading to eq. (1) is validated.

Fig. 4 shows the measured and the modeled series resistances for DUT-1. The strong frequency-dependency of the series resistance was observed for all test structures. While the series resistance was fixed in the conventional model without R_p shown in Fig. 2 [1], the proposed model very accurately describes the strong frequency-dependent series resistance. To demonstrate the capability of the proposed model, we have confirmed that the modeled *Q*-factor matched very well with the measured one as shown in Fig. 5. Fig. 6 shows the measured and the modeled *Y*-parameters, and excellent agreement between measurement and model up to 20 GHz was obtained.

3. Effect of Substrate Grounded Shields

Integrated passive devices have resistive components due to the lossy Si substrate. These resistances consume signal power and even generate thermal noise, and thus gain and noise performances of RF IC's are degraded [5]. To reduce such effects, grounded shields have been widely exploited. The experiments on various substrate conditions were performed with the proposed model. As shown in Fig. 7, metal-1, poly, and n+ diffusion shields were used, and the effect of d_p for unshielded capacitors was also examined. As a result, Table I indicates that grounded shields significantly reduce substrate resistance (R_{sub}) without any change of main capacitance (C_s). However, using metal-1 shield, C_{ox} was slightly larger, compared with using poly or n+ diffusion shield. In the case of unshielded capacitors, R_{sub} decreased as d_p decreased, but did not remarkably decreased as much as that of shielded capacitors.

4. Conclusions

In this paper, a simple lumped-element model for the MIM capacitor taking the frequency-dependent series resistance into account has been developed and verified over frequency up to 20 GHz through *S*-parameter measurements. In addition, based on various experimental results with the proposed model, to mitigate the effect of lossy silicon substrate, grounded shield should be used and poly or n+ diffusion shield was recommended.

Acknowledgements: This work was partially supported by the KOSEF through the MICROS center at KAIST and by the Samsung Advanced Institute of Technology.

References

[1] C. Zhen et al., *IEEE MWC Lett.* **12**, 246 (2002)
[2] C.-S. Yen et al., *Proc. IEEE* **70**, 750 (1982)
[3] T. Kamgaing et al., *IEEE MTT-S IMS Digest* (2002) p.153
[4] J. N. Burghartz et al., *IEEE TMTT* **44**, 100 (1996)
[5] R. Fujimoto et al., *IEEE JSSC* **37**, 852 (2002)

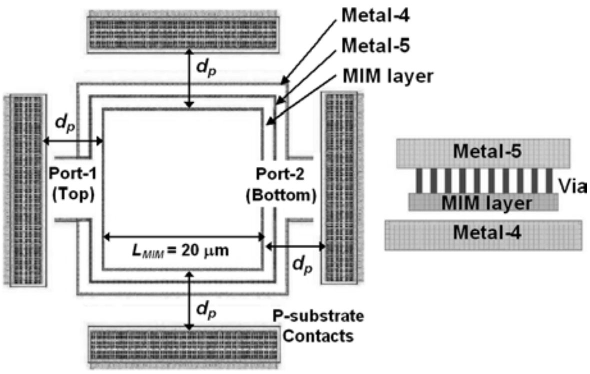

Fig. 1 Top (left) and cross (right) sectional views of an Metal -Insulator-Metal (MIM) capacitor. d_p is the distance from the edge of MIM layer to p-substrate contacts.

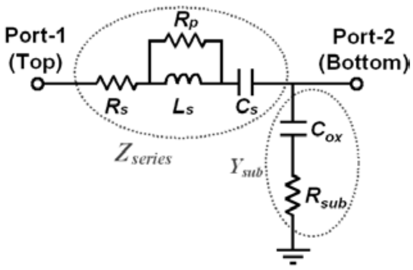

Fig. 2 Proposed equivalent circuit model of an MIM capacitor.

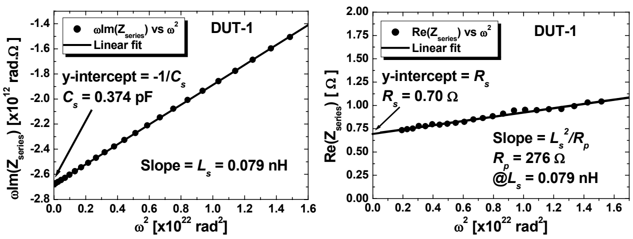

(a) (b)

Fig. 3 (a) Parameter extraction of L_s and C_s for the DUT-1. L_s and C_s were extracted from slope and y-intercept of ωIm(Z_{series}) versus ω^2, respectively. (b) Parameter extraction of R_p and R_s for the DUT-1. R_p and R_s were extracted from slope and y-intercept of Re(Z_{series}) versus ω^2, respectively.

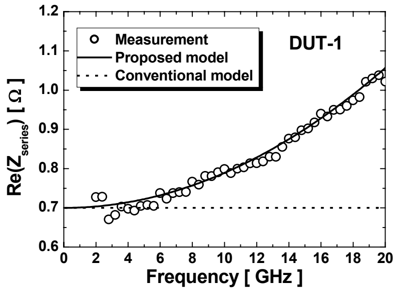

Fig. 4 Measured and modeled series resistances for the DUT-1.

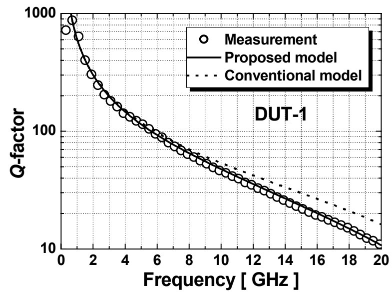

Fig. 5 Measured and modeled Q-factors for the DUT-1. Compared with the conventional model without R_p, a significant improvement was shown at high frequency region.

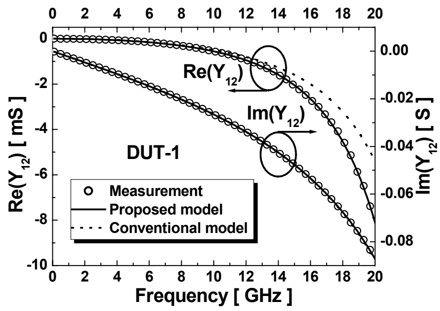

Fig. 6 Measured and modeled Y_{12} for the DUT-1. The Y-parameters of the proposed equivalent circuit model matched very well with those measured.

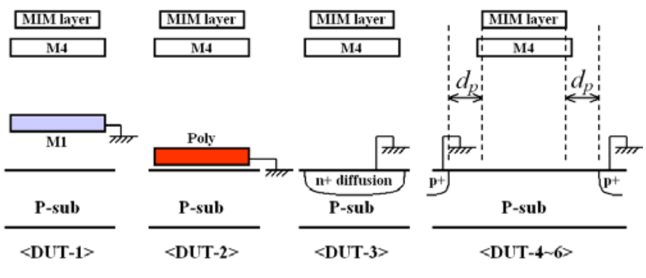

Fig. 7 Cross-sections of MIM capacitors from DUT-1 to DUT-6

Table I Extracted parameter values for MIM capacitors with different substrate conditions (Capacitor size: 20 × 20 μm^2)

	C_s [pF]	R_s [Ω]	R_p [Ω]	L_s [nH]	C_{ox} [fF]	R_{sub} [Ω]
DUT-1 (Metal-1 shield)	0.374	0.70	276	0.079	6.0	23
DUT-2 (Poly shield)	0.374	0.72	155	0.084	4.1	55
DUT-3 (N+ diffusion shield)	0.374	0.69	173	0.085	3.8	52
DUT-4 (No shield, d_p=10μm)	0.374	0.70	252	0.085	4.0	931
DUT-5 (No shield, d_p=20μm)	0.374	0.68	292	0.086	4.0	1169
DUT-6 (No shield, d_p=30μm)	0.374	0.68	300	0.088	4.1	1294
DUT-7 (No shield, No P-sub contact)	0.374	0.69	300	0.087	3.8	1614